



Cite this: *RSC Adv.*, 2017, 7, 52588

# Core-shell structured NaMnF<sub>3</sub>: Yb, Er nanoparticles for bioimaging applications†

Shuai Ye,  Mengjie Zhao, Jun Song \* and Junle Qu\*

NaMnF<sub>3</sub>: Yb,Er upconversion nanoparticles (UCNPs) have received considerable attention due to their single-band emission. In this paper, a modified thermal decomposition method to synthesize single or core/shell structured lanthanide-doped NaMnF<sub>3</sub> nanoparticles is proposed. The NaMnF<sub>3</sub>: 20% Yb<sup>3+</sup>, 2% Er<sup>3+</sup> nanoparticles displayed pure red emission under 980 nm laser excitation, and the emission intensity could be significantly enhanced by coating a NaMnF<sub>3</sub> or NaMnF<sub>3</sub>: 20% Yb<sup>3+</sup> shell layer on their surfaces. Moreover, NaMnF<sub>3</sub>: 20% Yb<sup>3+</sup>, 2% Er<sup>3+</sup> nanoparticles shelled with NaMnF<sub>3</sub>: 20% Nd<sup>3+</sup> or NaMnF<sub>3</sub>: 20% Yb<sup>3+</sup>, 20% Nd<sup>3+</sup> were synthesized for the first time, and displayed pure red emission when excited by an 808 nm laser. The core/shell structured NaMnF<sub>3</sub>: Yb/Er@NaMnF<sub>3</sub>: Yb or NaMnF<sub>3</sub>: Yb/Er@NaMnF<sub>3</sub>: Yb/Nd nanoparticles were applied to bioimaging. The NaMnF<sub>3</sub> based UCNPs exhibited good photostability and biocompatibility in HeLa cells. The obtained images indicated that the UCNPs could mainly exist in the cytoplasmic regions in the cells. Besides, images from the same region exposed to laser irradiations at 808 nm and 980 nm were found to be comparable. This result indicated that, for NaMnF<sub>3</sub>: 20% Yb<sup>3+</sup>, 2% Er<sup>3+</sup>@NaMnF<sub>3</sub>: 20% Yb<sup>3+</sup>, 20% Nd<sup>3+</sup> nanoparticles, laser excitation at 808 nm was as efficient as that at 980 nm for bioimaging.

Received 19th September 2017

Accepted 6th November 2017

DOI: 10.1039/c7ra10393j

rsc.li/rsc-advances

## 1. Introduction

Lanthanide-doped upconversion nanoparticles (UCNPs) have received considerable attention due to their intriguing features including non-autofluorescence, low photobleaching, strong penetration abilities, and low toxicity.<sup>1–10</sup> UCNPs have been widely used in solar cells, biolabeling, bioimaging, optical data storage, drug delivery, *etc.*<sup>11–15</sup> UCNPs with red single-band emission are preferred for biological imaging applications, as red light can penetrate deeper than other visible wavelengths through most tissues.<sup>16,17</sup> Besides, UCNPs with only red single-band emission are ideal candidates for photodynamic therapy applications, as the absorption peak of most commercial photosensitizers is located in the red region at ~650–670 nm.<sup>18,19</sup> Therefore, to satisfy the requirements of several applications, the synthesis of UCNPs with pure red emission is crucial.<sup>20</sup>

Until now, most research studies on the synthesis of UCNPs with strong red or near-infrared (NIR) emission have focused on Yb/Er or Yb/Tm doped NaYF<sub>4</sub> nanoparticles, as strong green (~540 nm) and weak red (~654 nm) emissions are produced by Yb/Er doped NaYF<sub>4</sub> nanoparticles, whereas blue (~480 nm) and strong NIR (~800 nm) emissions are produced by Yb/Tm doped

NaYF<sub>4</sub> nanoparticles.<sup>21–24</sup> Although each trivalent lanthanide activator ion has a unique energy level structure to produce emission peaks at specific wavelengths, the excitation and relaxation dynamics of energy levels involved in UC processes can be manipulated to vary the relative luminescence intensity between different UC bands.<sup>25–32</sup> The UC emission color may be tuned by incorporating other ions such as Mn<sup>2+</sup>, Zr<sup>4+</sup>, Mg<sup>2+</sup> or Ce<sup>3+</sup> in the host lattice.<sup>33–38</sup> Mn<sup>2+</sup> ion doped NaYF<sub>4</sub> nanoparticles show very promising performances, because the <sup>4</sup>T<sub>1</sub> energy states of Mn<sup>2+</sup> ions can facilitate non-radiative energy transfer from the <sup>2</sup>H<sub>9/2</sub> and <sup>4</sup>S<sub>3/2</sub> levels to the <sup>4</sup>F<sub>9/2</sub> level of Er<sup>3+</sup> ions (from <sup>1</sup>D<sub>2</sub> and <sup>1</sup>G<sub>4</sub> levels to <sup>3</sup>F<sub>4</sub> levels of Tm<sup>3+</sup> ions), which can tune the color emission from green to red or from blue to NIR for the Yb/Er and Yb/Tm doped UCNPs, respectively. Thus, UCNPs with single red or NIR band emissions can be obtained.

Besides, UCNPs with Yb<sup>3+</sup> as sensitizer are generally excited by a 980 nm laser. However, the use of 980 nm NIR photons has an intrinsic disadvantage due to the strong absorption of water molecules in biological tissues at that wavelength, resulting in the risk of local temperature rise or even tissue overheating under continual irradiation.<sup>39–41</sup> To avoid water absorption in tissues, the wavelength of the exciting light source should be shorter than 800 nm. A promising strategy was proposed to incorporate Nd<sup>3+</sup> ions into UCNPs as sensitizers to absorb the energy of the 800 nm photons, followed by transfer of non-radiative energy to Yb<sup>3+</sup> ions.<sup>42</sup> Owing to the quenching effect between them, Nd<sup>3+</sup> and activator ions (Er<sup>3+</sup>, Tm<sup>3+</sup>) needed to be separated by a core/shell structure to obtain effective Nd<sup>3+</sup> sensitized UCNPs.<sup>43,44</sup>

Key Lab of Optoelectronic Devices and Systems of Ministry of Education/Guangdong Province, College of Optoelectronic Engineering, Shenzhen University, Shenzhen 518060, China. E-mail: songjun@szu.edu.cn; jlqu@szu.edu.cn

† Electronic supplementary information (ESI) available. See DOI: 10.1039/c7ra10393j

To maintain the penetration depth and simultaneously avoid overheating during *in vivo* bioimaging, it was necessary to develop UCNP which can upconvert from  $\sim 800$  nm NIR laser to red light. Obviously,  $\text{Nd}^{3+}$  sensitized  $\text{NaMnF}_3$ : Yb/Er nanoparticles were the most promising candidate, although  $\text{Nd}^{3+}$  sensitized  $\text{Ho}^{3+}$  single band UCNP have been reported.<sup>45</sup> Until now, solvothermal routes have been typically used to synthesize  $\text{NaMnF}_3$ : Yb/Er nanoparticles;<sup>46,47</sup> the syntheses have been conducted in teflon-lined autoclaves under high pressure, and core/shell UCNP with perfect morphologies have been hardly obtained. In this work, a novel method to synthesize single or core/shell structured  $\text{NaMnF}_3$ : Yb, Er nanoparticles with pure red emission under 808 or 980 nm laser excitation for bioimaging was developed. Then, bioimaging of core/shell structured  $\text{NaMnF}_3$ : Yb/Er nanoparticles in HeLa cells was investigated.

## 2. Experimental

### 2.1 Materials

For the proposed procedure, appropriate selection of the raw materials is critical.  $\text{MnCl}_2$  hardly reacts with oleic acid to produce the necessary metal-oleic complex. The frequently used rare earth chloride must be abandoned, because chloride ions could hinder the complex reaction of  $\text{Mn}^{2+}$  ions. Rather, rare earth acetate hexahydrate and manganese(II) pentanedionate were used. Chemicals were purchased from Alfa Aesar and used without further purification. The acetate hexahydrate had a trace metal basis of 99.9%.

### 2.2 Synthesis of single nanoparticles

In this work,  $\text{NaMnF}_3$ : 20%  $\text{Yb}^{3+}$ , A (A =  $\text{Er}^{3+}$ ,  $\text{Ho}^{3+}$ , or  $\text{Tm}^{3+}$ ) nanoparticles were prepared by a modified one-step thermal decomposition. A mixture containing 0.2 mmol of  $\text{Yb}(\text{CH}_3\text{COO})_3 \cdot 4\text{H}_2\text{O}$ ,  $(0.8 - x)$  mmol of manganese(II) pentanedionate, and  $x$  mmol of  $\text{A}(\text{CH}_3\text{COO})_3 \cdot 4\text{H}_2\text{O}$  was placed in a 100 ml flask. Then, 7 ml of oleic acid and 15 ml of 1-octadecene were added, and the solution was heated to 160 °C for 60 min under Ar atmosphere and vigorous stirring. After cooling to room temperature, a solution comprising 4 mmol of  $\text{NH}_4\text{F}$  and 2.5 mmol of NaOH in 10 ml of methanol was added, and the mixture was heated to 100 °C for 30 min to evaporate methanol. Finally, the solution was heated to 300 °C under Ar atmosphere for 60 min, and then cooled to room temperature. The nanoparticles were precipitated with 50 ml of ethanol, collected after centrifugation (7000 rpm, 5 min), and redispersed in 10 ml of hexane for later use.

### 2.3 Synthesis of core/shell structured nanoparticles

To prepare core/shell structured  $\text{NaMnF}_3$ : 20%  $\text{Yb}^{3+}$ , A nanoparticles, 0.5 mmol of manganese(II) pentanedionate was added to a 100 ml flask, followed by 7 ml of oleic acid and 15 ml of 1-octadecene. The solution was heated to 160 °C for 60 min under Ar atmosphere and vigorous stirring. After cooling to room temperature, 5 ml of colloidal  $\text{NaMnF}_3$ : 20%  $\text{Yb}^{3+}$ /A, synthesized as in Section 2.2, was added, followed by a solution

consisting of 2 mmol of  $\text{NH}_4\text{F}$  and 1.25 mmol of NaOH in 5 ml of methanol; the mixture was then heated to 100 °C for 30 min to evaporate methanol and hexane. Finally, the solution was heated to 290 °C under Ar atmosphere for 60 min, and subsequently cooled to room temperature. The nanoparticles were precipitated with 50 ml of ethanol, collected after centrifugation (7000 rpm, 5 min), and redispersed in 5 ml of hexane for characterization.

### 2.4 Surface modification of oleic acid (OA) UCNP by polymethacrylamide (PAAM)

To obtain hydrophilic UCNP for biological application, PAAM was used to modify OA-capped UCNP. Firstly, 0.5 ml of a solution of hexane-dispersed OA-UCNP was added to 5 ml of anhydrous ethanol containing 0.5 ml of PAAM, and stirred vigorously at ambient temperature for 24 h. The UCNP were precipitated by centrifugation (10 000 rpm; 15 min) and redispersed in phosphate buffer saline solution by sonication for further research.

### 2.5 Characterization

The sample morphologies were observed by transmission electron microscopy (TEM; Joel JEM-2100; acceleration voltage: 200 kV). The UC luminescence spectra were recorded using an Ocean Optics QE65000 spectrofluorometer with a slit width defining a spectral resolution of 1 nm. The colloidal UCNP were excited at 980 or 808 nm by using a continuous-wave laser diode with tunable laser power in the scale of 0–0.8 W. The spectra of colloidal UCNP were measured with 0.5 W laser irradiation if no special requirement was mentioned. The emission decay time was measured by using the proposed system illustrated in.<sup>48</sup>

## 3. Results and discussion

Fig. 1a shows the TEM morphologies of the synthesized  $\text{NaMnF}_3$ : 20%  $\text{Yb}^{3+}$ , 2%  $\text{Er}^{3+}$  nanoparticles. Ultrasmall lanthanide-doped  $\text{NaMnF}_3$  nanoparticles were synthesized following the proposed procedure; all the nanoparticles were uniformly monodispersed. The average size of the  $\text{NaMnF}_3$ : 20%  $\text{Yb}^{3+}$ , 2%  $\text{Er}^{3+}$  nanoparticles was approximately 9.5 nm. The XRD pattern shown in Fig. S1† was in accord with the standard  $\text{NaMnF}_3$  host lattice of JCPDS 18-1224, indicating the prepared UCNP were  $\text{NaMnF}_3$  phase. Fig. 1b shows the UC emission spectrum of the as-synthesized  $\text{NaMnF}_3$ : 20%  $\text{Yb}^{3+}$ , 2%  $\text{Er}^{3+}$  nanoparticles. Only a single emission band centered at 654 nm, which corresponds to the energy transfer  $^4\text{F}_{9/2} \rightarrow ^4\text{F}_{15/2}$  of  $\text{Er}^{3+}$  ions, is visible in the spectrum. The emission band corresponding to the energy transfer  $^4\text{S}_{3/2} \rightarrow ^4\text{F}_{15/2}$  of  $\text{Er}^{3+}$  ions—present in the  $\text{NaYF}_4$ : 20%  $\text{Yb}^{3+}$ , 2%  $\text{Er}^{3+}$  nanoparticle spectrum—completely disappears in the  $\text{NaMnF}_3$ : 20%  $\text{Yb}^{3+}$ , 2%  $\text{Er}^{3+}$  nanoparticle spectrum. This is ascribed to the non-radiative energy transfer from the  $^4\text{S}_{3/2}$  level of  $\text{Er}^{3+}$  ions to the  $^4\text{T}_1$  level of  $\text{Mn}^{2+}$  ions, followed by back energy transfer to the  $^4\text{F}_{9/2}$  level of  $\text{Er}^{3+}$  ions. Hence, the color output of the  $\text{NaMnF}_3$ : 20%  $\text{Yb}^{3+}$ , 2%  $\text{Er}^{3+}$  nanoparticles is pure red, as shown in



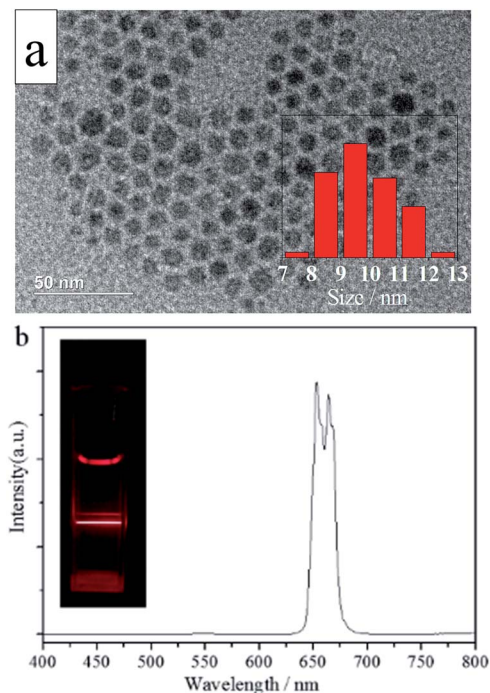


Fig. 1 (a) Typical TEM image and (b) photoluminescence spectrum of NaMnF<sub>3</sub>: 20% Yb<sup>3+</sup>, 2% Er<sup>3+</sup> nanoparticles. The inset in (a) shows the size distribution of NaMnF<sub>3</sub>: 20% Yb<sup>3+</sup>, 2% Er<sup>3+</sup> nanoparticles.

Fig. S2.† Additionally, Yb/Ho and Yb/Tm doped NaMnF<sub>3</sub> nanoparticles were synthesized. TEM images and emission spectra are shown in Figs. S3 and S4.† The Yb/Ho and Yb/Tm doped NaMnF<sub>3</sub> nanoparticles were also monodispersed with average sizes of approximately 9.5 and 9.8 nm, respectively. The NaMnF<sub>3</sub>: 20% Yb<sup>3+</sup>, 1% Tm<sup>3+</sup> nanoparticles displayed a single-band emission centered at 800 nm, corresponding to the energy transfer <sup>3</sup>H<sub>4</sub> → <sup>3</sup>H<sub>6</sub>. However, the NaMnF<sub>3</sub>: 20% Yb<sup>3+</sup>, 2% Ho<sup>3+</sup> nanoparticles exhibited a multiband output including a weak green emission band at 540 nm and a strong emission band at 640 nm.

Notably, the UC emission intensity can be significantly enhanced by coating effective shell layers on the surface of the UCNPs.<sup>4,49</sup> Layers of different types (*i.e.*, an inert NaMnF<sub>3</sub> layer or an active NaMnF<sub>3</sub>: 20% Yb<sup>3+</sup> layer) were coated on the surfaces of NaMnF<sub>3</sub>: 20% Yb<sup>3+</sup>, 2% Er<sup>3+</sup> nanoparticles to boost the UC emission intensity, as shown in Fig. 2. The red emission intensity was enhanced by a factor of 1.75 in the presence of the inert NaMnF<sub>3</sub> layer, whereas an enhancement factor of 3 was obtained by coating with the active NaMnF<sub>3</sub>: 20% Yb<sup>3+</sup> layer. The output color of all these coated nanoparticles was red, as shown in the inset images; however, a very weak peak centered at 540 nm appeared in the spectrum of the NaMnF<sub>3</sub>: 20% Yb<sup>3+</sup>, 2% Er<sup>3+</sup>@NaMnF<sub>3</sub>: 20% Yb<sup>3+</sup> nanoparticles, whose TEM image is shown in Fig. 2b. The average size was approximately 16 nm, almost twice that of the NaMnF<sub>3</sub>: 20% Yb<sup>3+</sup>, 2% Er<sup>3+</sup> nanoparticles.

To investigate the mechanism behind the intensity enhancement of the red emission in core/shell structured lanthanide-doped NaMnF<sub>3</sub> nanoparticles, the dependence of the red emission intensity on the pump laser power was

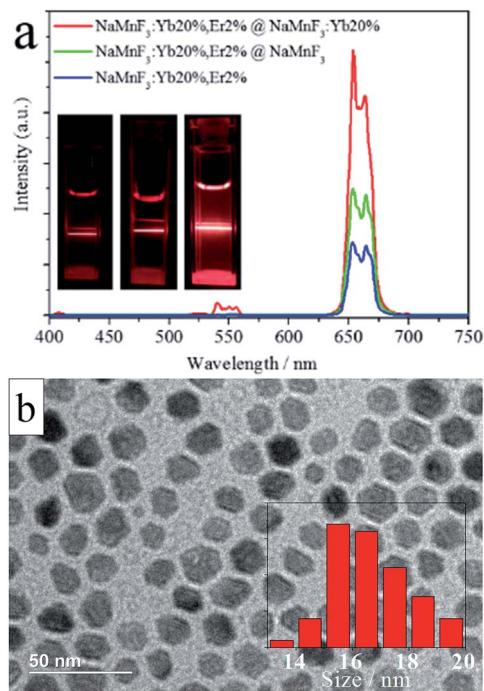


Fig. 2 (a) Spectra of NaMnF<sub>3</sub>: 20% Yb<sup>3+</sup>, 2% Er<sup>3+</sup> nanoparticles with and without shell layers; the inset shows the photographs of the nanoparticles (left to right: NaMnF<sub>3</sub>: 20% Yb<sup>3+</sup>, 2% Er<sup>3+</sup>; NaMnF<sub>3</sub>: 20% Yb<sup>3+</sup>, 2% Er<sup>3+</sup>@NaMnF<sub>3</sub>; NaMnF<sub>3</sub>: 20% Yb<sup>3+</sup>, 2% Er<sup>3+</sup>@NaMnF<sub>3</sub>: 20% Yb<sup>3+</sup>). (b) Typical TEM image of NaMnF<sub>3</sub>: 20% Yb<sup>3+</sup>, 2% Er<sup>3+</sup>@NaMnF<sub>3</sub>: 20% Yb<sup>3+</sup> nanoparticles; the inset shows the size distribution of NaMnF<sub>3</sub>: 20% Yb<sup>3+</sup>, 2% Er<sup>3+</sup>@NaMnF<sub>3</sub>: 20% Yb<sup>3+</sup> nanoparticles.

measured for NaMnF<sub>3</sub>: 20% Yb<sup>3+</sup>, 2% Er<sup>3+</sup> nanoparticles with or without shell layer (Fig. 3). Generally, the number of photons required to populate the upper emitting state under unsaturated conditions is related to the intensity by:

$$I_f \propto P^n \quad (1)$$

where  $I_f$  is the photoluminescence intensity,  $P$  is the pump laser power, and  $n$  is the number of laser photons required. The

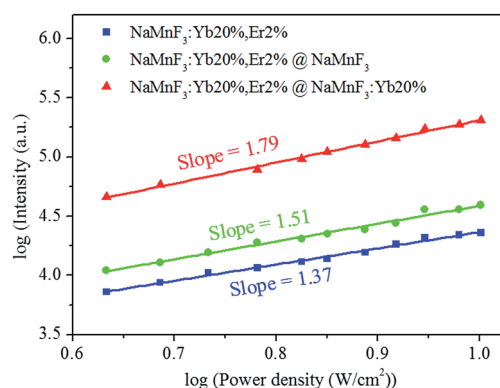


Fig. 3 Dependence of red emission intensity on laser pumping power for NaMnF<sub>3</sub>: 20% Yb<sup>3+</sup>, 2% Er<sup>3+</sup>, NaMnF<sub>3</sub>: 20% Yb<sup>3+</sup>, 2% Er<sup>3+</sup>@NaMnF<sub>3</sub>, and NaMnF<sub>3</sub>: 20% Yb<sup>3+</sup>, 2% Er<sup>3+</sup>@NaMnF<sub>3</sub>: 20% Yb<sup>3+</sup> nanoparticles.





slopes of the red-emission bands of the NaMnF<sub>3</sub>: 20% Yb<sup>3+</sup>, 2% Er<sup>3+</sup>, NaMnF<sub>3</sub>: 20% Yb<sup>3+</sup>, 2% Er<sup>3+</sup>@NaMnF<sub>3</sub>, and NaMnF<sub>3</sub>: 20% Yb<sup>3+</sup>, 2% Er<sup>3+</sup>@NaMnF<sub>3</sub>: 20% Yb<sup>3+</sup> nanoparticles were 1.37, 1.51, and 1.79, respectively, indicating that the red emission involved a two-photon process in all these cases. Additionally, the enhanced slope of the shell-structured nanoparticles indicated that the shell layer was suppressing surface-related quenching effects.

The decay profiles of the <sup>4</sup>S<sub>3/2</sub> → <sup>4</sup>F<sub>15/2</sub> transition of Er<sup>3+</sup> ions at 540 nm and <sup>4</sup>F<sub>9/2</sub> → <sup>4</sup>F<sub>15/2</sub> transition of Er<sup>3+</sup> ions at 654 nm were also measured, as shown in Fig. 4. The decay curves were non-exponential, owing to enhanced non-radiative energy transfer processes, as well as effects of the surrounding environment. The effective lifetime  $\tau_m$  is

$$\tau = \frac{\int_0^{\infty} tI(t)dt}{\int_0^{\infty} I(t)dt} \quad (2)$$

where  $I(t)$  is the intensity at time  $t$ . The effective decay times for the <sup>4</sup>S<sub>3/2</sub> and <sup>4</sup>F<sub>9/2</sub> states of Er<sup>3+</sup> ions in NaMnF<sub>3</sub>: 20% Yb<sup>3+</sup>, 2% Er<sup>3+</sup> nanoparticles were 19.7 and 34.0  $\mu$ s, respectively, which were significantly prolonged in NaMnF<sub>3</sub> shelled nanoparticles. The prolonged lifetime was mainly attributed to the suppression of surface-related quenching effects. The NaMnF<sub>3</sub>: 20% Yb<sup>3+</sup> shell layer could not completely suppress the quenching effect, but it enhanced the absorption of the 980 nm excitation laser. Thus, the lifetime of the NaMnF<sub>3</sub>: 20% Yb<sup>3+</sup>, 2%

Er<sup>3+</sup>@NaMnF<sub>3</sub>: 20% Yb<sup>3+</sup> nanoparticles was longer. The appearance of the green emission at 540 nm in the NaMnF<sub>3</sub>: 20% Yb<sup>3+</sup>, 2% Er<sup>3+</sup>@NaMnF<sub>3</sub>: 20% Yb<sup>3+</sup> nanoparticle spectrum (Fig. 2) was related to the segregation of Yb<sup>3+</sup> ions at the interface between core and shell, as the coating of the NaMnF<sub>3</sub>: 20% Yb<sup>3+</sup> shell layer increased the concentration of Yb<sup>3+</sup> activator ions at the interface.

The NaMnF<sub>3</sub>: 20% Yb<sup>3+</sup>, 2% Er<sup>3+</sup>@NaMnF<sub>3</sub>: 20% Yb<sup>3+</sup> nanoparticles were applied to bioimaging, as shown in Fig. 5. HeLa cells were incubated with PAAM-UCNPs for 4 h. After washing the unbound nanoparticles, the HeLa cells were imaged in bright field and fluorescence field by using a Leica confocal microscope equipped with a 980 nm NIR laser. Clear red UC luminescence from the UCNPs under 980 nm excitation (Fig. 5a) and green downconversion fluorescence from the DNA staining dye (SYTO®11, Invitrogen) under 514 nm excitation (Fig. 5b) were simultaneously observed in the HeLa cells. The merged images (Fig. 5c) show that the UCNP fluorescence mainly occurred in the cytoplasmic regions. Furthermore, the toxicity of the PAAM-UCNPs was investigated in HeLa cells, as shown in Fig. S5.† After 24 h of incubation in PAAM-UCNPs with different concentrations, the cell viability was still above 80% for UCNP concentrations up to 400  $\mu$ g ml<sup>-1</sup>, indicating a good biocompatibility of the NaMnF<sub>3</sub>: 20% Yb<sup>3+</sup>, 2% Er<sup>3+</sup>@NaMnF<sub>3</sub>: 20% Yb<sup>3+</sup> nanoparticles with the cells. The photostability of the PAAM-UCNPs was also measured, as shown in Fig. S6.† The photoluminescence intensity of the NaMnF<sub>3</sub>: 20% Yb<sup>3+</sup>, 2% Er<sup>3+</sup>@NaMnF<sub>3</sub>: 20% Yb<sup>3+</sup> nanoparticles was reduced by only 2.3% after irradiation for 10 min.

In addition, NaMnF<sub>3</sub>: 20% Yb<sup>3+</sup>, 2% Er<sup>3+</sup> nanoparticles shelled with Nd<sup>3+</sup> sensitized layers (NaMnF<sub>3</sub>: 20% Nd<sup>3+</sup> or

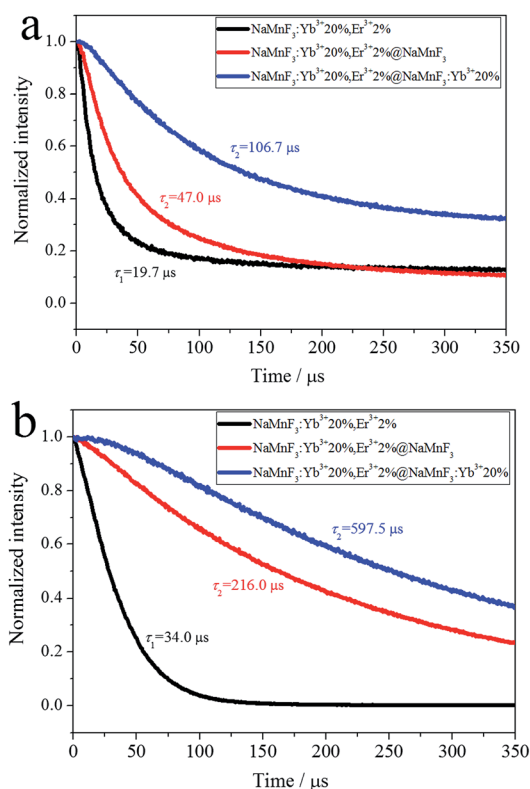


Fig. 4 Decay profiles of transitions of Er<sup>3+</sup> ions: (a) <sup>4</sup>S<sub>3/2</sub> → <sup>4</sup>I<sub>15/2</sub> at 540 nm and (b) <sup>4</sup>F<sub>9/2</sub> → <sup>4</sup>I<sub>15/2</sub> at 654 nm.

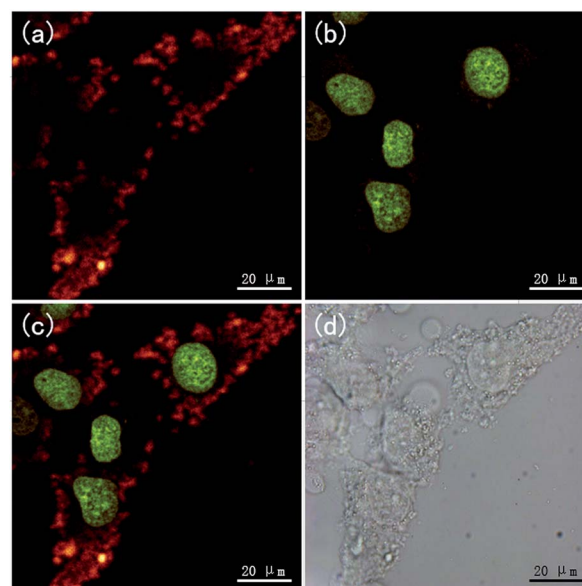


Fig. 5 (a) Upconversion luminescence image of UCNPs (NaMnF<sub>3</sub>: 20% Yb<sup>3+</sup>, 2% Er<sup>3+</sup>@NaMnF<sub>3</sub>: 20% Yb<sup>3+</sup> nanoparticles) in HeLa cells ( $\lambda_{ex}$  = 980 nm). (b) Fluorescence image of DNA staining dye ( $\lambda_{ex}$  = 514 nm). (c) Merged fluorescence image of UCNPs (red) and DNA staining dye (green). (d) Bright field image.



NaMnF<sub>3</sub>: 20% Yb<sup>3+</sup>, 20% Nd<sup>3+</sup>) were synthesized to obtain pure red emission under 808 nm laser excitation; the photoluminescence spectra are shown in Fig. 6. The NaMnF<sub>3</sub>: 20% Yb<sup>3+</sup>, 2% Er<sup>3+</sup> nanoparticles shelled with Nd<sup>3+</sup> sensitized layers exhibited pure red emission when excited by 808 nm or 980 nm laser. However, the NaMnF<sub>3</sub>: 20% Yb<sup>3+</sup>, 2% Er<sup>3+</sup>@NaMnF<sub>3</sub>: 20% Yb<sup>3+</sup>, 20% Nd<sup>3+</sup> nanoparticles exhibited considerably higher emission intensity than the NaMnF<sub>3</sub>: 20% Yb<sup>3+</sup>, 2% Er<sup>3+</sup>@NaMnF<sub>3</sub>: 20% Nd<sup>3+</sup> nanoparticles under 808 nm laser excitation, which indicated that the incorporation of Yb<sup>3+</sup> ions into the Nd<sup>3+</sup> sensitized shell could facilitate the energy transfer from Nd<sup>3+</sup> to Yb<sup>3+</sup> ions.<sup>39,44</sup> The TEM image of the NaMnF<sub>3</sub>: 20% Yb<sup>3+</sup>, 2% Er<sup>3+</sup>@NaMnF<sub>3</sub>: 20% Yb<sup>3+</sup>, 20% Nd<sup>3+</sup> nanoparticles is shown in Fig. S7.† The average size was approximately 17 nm.

The NaMnF<sub>3</sub>: 20% Yb<sup>3+</sup>, 2% Er<sup>3+</sup>@NaMnF<sub>3</sub>: 20% Yb<sup>3+</sup>, 20% Nd<sup>3+</sup> nanoparticles were also applied to bioimaging, as shown in Fig. 7. The HeLa cells incubated with PAAM-UCNPs were imaged in bright field and fluorescence field by using a Leica confocal microscope equipped with 808 nm and 980 nm NIR lasers. The merged images (Fig. 7d and e) indicate that the UCNPs fluorescence mainly occurred in the cytoplasmic regions. The images obtained for the same region by using 808 nm and 980 nm laser excitations (Fig. 7a and b) appear comparable, which implied that, for NaMnF<sub>3</sub>: 20% Yb<sup>3+</sup>, 2% Er<sup>3+</sup>@NaMnF<sub>3</sub>: 20% Yb<sup>3+</sup>, 20% Nd<sup>3+</sup> nanoparticles, the 808 nm laser excitation was as efficient as the 980 nm laser excitation for bioimaging. Notably, it has been confirmed<sup>39,43</sup> that, compared with the

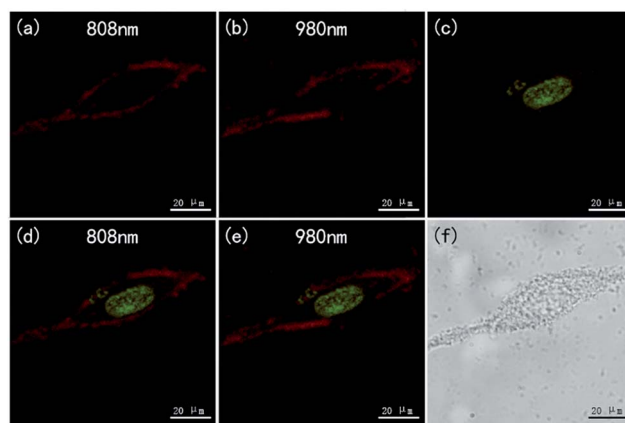


Fig. 7 (a) Upconversion luminescence image of UCNPs (NaMnF<sub>3</sub>: 20% Yb<sup>3+</sup>, 2% Er<sup>3+</sup>@NaMnF<sub>3</sub>: 20% Yb<sup>3+</sup>, 20% Nd<sup>3+</sup> nanoparticles) in HeLa cells ( $\lambda_{\text{ex}}$  = 808 nm); (b) upconversion luminescence image of UCNPs in HeLa cells ( $\lambda_{\text{ex}}$  = 980 nm); (c) fluorescence image of DNA staining dye ( $\lambda_{\text{ex}}$  = 514 nm); (d) merged fluorescence image of UCNPs (red,  $\lambda_{\text{ex}}$  = 808 nm) and DNA staining dye (green); (e) merged fluorescence image of UCNPs (red,  $\lambda_{\text{ex}}$  = 980 nm) and DNA staining dye (green); (f) bright field image.

popular excitation wavelength of 980 nm, the 808 nm excitation wavelength minimized the overheating effect for *in vivo* tissues.

## 4. Conclusions

A novel strategy was proposed to synthesize single or core/shell structured lanthanide-doped NaMnF<sub>3</sub> nanoparticles. The synthesized NaMnF<sub>3</sub>: 20% Yb<sup>3+</sup>, 2% Er<sup>3+</sup> nanoparticles displayed pure red emission under 980 nm laser excitation, and the luminescence intensity could be significantly enhanced by coating their surface with a NaMnF<sub>3</sub>: 20% Yb<sup>3+</sup> shell layer. Moreover, NaMnF<sub>3</sub>: 20% Yb<sup>3+</sup>, 2% Er<sup>3+</sup> nanoparticles shelled with NaMnF<sub>3</sub>: 20% Yb<sup>3+</sup>, 20% Nd<sup>3+</sup> were synthesized, and displayed pure red emission under 808 nm laser excitation. The NaMnF<sub>3</sub>: 20% Yb<sup>3+</sup> NaMnF<sub>3</sub>: 20% Yb<sup>3+</sup>, 20% Nd<sup>3+</sup> were applied to bioimaging under excitation of 808 nm and 980 nm laser excitations, revealing that the laser excitation at 808 nm was as efficient as that at 980 nm.

## Conflicts of interest

There are no conflicts to declare.

## Acknowledgements

Parts of this work were supported by the National Basic Research Program of China (2015CB352005); the National Natural Science Foundation of China (61605124/61525503/61378091/ 61405123/61405062); Guangdong Natural Science Foundation Innovation Team (2014A030312008); Hong Kong, Macao and Taiwan cooperation innovation platform & major projects of international cooperation in Colleges and Universities in Guangdong Province (2015KGJHZ002); and Shenzhen Basic Research Project (JCYJ20150324141711561/

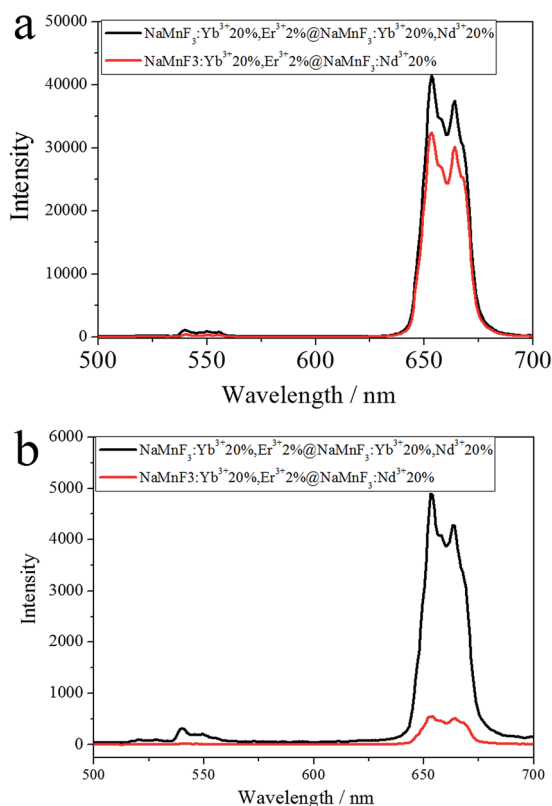


Fig. 6 Spectra of NaMnF<sub>3</sub>: 20% Yb<sup>3+</sup>, 2% Er<sup>3+</sup> nanoparticles shelled with Nd<sup>3+</sup> sensitized layers excited by (a) 980 nm or (b) 808 nm laser.



JCYJ2015093010 4948169/ZDSYS20140430164957663/KQCX20140509172719 305); the Training Plan of Guangdong Province Outstanding Young Teachers in Higher Education Institutions (Yq2013142).

## References

- G. Chen, H. Qiu, P. N. Prasad and X. Chen, Upconversion Nanoparticles: Design, Nanochemistry, and Applications in Theranostics, *Chem. Rev.*, 2014, **114**, 5161–5214.
- X. Liu, R. Deng, Y. Zhang, Y. Wang, H. Chang, L. Huang and X. Liu, Probing the Nature of Upconversion Nanocrystals: Instrumentation Matters, *Chem. Soc. Rev.*, 2015, **44**, 1479–1508.
- W. Zheng, P. Huang, D. Tu, E. Ma, H. Zhu and X. Chen, Lanthanide-doped Upconversion Nano-bioprobes: Electronic Structures, Optical Properties and Biodetection, *Chem. Soc. Rev.*, 2015, **44**, 1379–1415.
- G. Chen, H. Ågren, T. Y. Ohulchanskyya and P. N. Prasad, Light Upconverting Core-shell Nanostructures: Nanophotonic Control for Emerging Applications, *Chem. Soc. Rev.*, 2015, **44**, 1680–1713.
- X. Li, F. Zhang and D. Zhao, Lab on Upconversion Nanoparticles: Optical Properties and Applications Engineering via Designed Nanostructure, *Chem. Soc. Rev.*, 2015, **44**, 1346–1378.
- H. Dong, S. Du, X. Zheng, G. Lu, L. Sun, L. Li, P. Zhang, C. Zhang and C. Yan, Lanthanide Nanoparticles: From Design toward Bioimaging and Therapy, *Chem. Rev.*, 2015, **115**(19), 10725–10815.
- Y. Sun, W. Feng, P. Yang, C. Huang and F. Li, The Biosafety of Lanthanide Upconversion Nanomaterials, *Chem. Soc. Rev.*, 2015, **44**, 1509–1525.
- S. Gai, C. Li, P. Yang and J. Lin, Recent Progress in Rare Earth Micro/Nanocrystals: Soft Chemical Synthesis, Luminescent Properties, and Biomedical Applications, *Chem. Rev.*, 2014, **114**, 2343–2389.
- X. Liu, C. Yan and J. A. Capobianco, Photon Upconversion Nanomaterials, *Chem. Soc. Rev.*, 2015, **44**, 1299–1301.
- N. M. Idris, M. K. G. Jayakumar, A. Bansal and Y. Zhang, Upconversion nanoparticles as versatile light nanotransducers for photoactivation applications, *Chem. Soc. Rev.*, 2015, **44**, 1449–1478.
- A. Paulino, O. Olalla, M. Diego, L. Enrique, B. Isabel and R. Jorge, Synthesis, Characterization, and Application in HeLa Cells of an NIR Light Responsive Doxorubicin Delivery System Based on NaYF<sub>4</sub>:Yb, Tm@SiO<sub>2</sub>-PEG Nanoparticles, *ACS Appl. Mater. Interfaces*, 2015, **7**, 14992–14999.
- J. Shen, L. Zhao and G. Han, Lanthanide-doped Upconverting Luminescent Nanoparticle Platforms for Optical Imaging-guided Drug Delivery and Therapy, *Adv. Drug Delivery Rev.*, 2013, **5**, 744–755.
- L. Xiong, T. Yang, Y. Yang, C. Xu and F. Li, Long-term in vivo Biodistribution Imaging and Toxicity of Polyacrylic Acid-coated Upconversion Nanophosphors, *Biomaterials*, 2010, **3**, 7078–7085.
- Q. Zhan, X. Zhang, Y. Zhao, J. Liu and S. He, Tens of Thousands-fold Upconversion Luminescence Enhancement Induced by a Single Gold Nanorod, *Laser Photonics Rev.*, 2015, **9**, 479–487.
- G. Tian, X. Zheng, X. Zhang, W. Yin, J. Yu, D. Wang, Z. Zhang, X. Yang, Z. Gu and Y. Zhao, TPGS-stabilized NaYbF<sub>4</sub>:Er Upconversion Nanoparticles for Dual-modal Fluorescent/CT Imaging and Anticancer Drug Delivery to Overcome Multi-drug Resistance, *Biomaterials*, 2015, **8**, 107–116.
- G. Chen, J. Shen, T. Ohulchanskyy, N. J. Patel, A. Kutikov, Z. Li, J. Song, R. Pandey, H. Agren, P. Prasad and G. Han, ( $\alpha$ -NaYbF<sub>4</sub>:Tm<sup>3+</sup>)/CaF<sub>2</sub> Core/Shell Nanoparticles with Efficient Near-Infrared to Near-Infrared Upconversion for High-Contrast Deep Tissue Bioimaging, *ACS Nano*, 2012, **9**, 8280–8287.
- L. Zhou, R. Wang, C. Yao, X. Li, C. Wang, X. Zhang, C. Xu, A. Zeng, D. Zhao and F. Zhang, Single-band upconversion nanoprobe for multiplexed simultaneous *in situ* molecular mapping of cancer biomarkers, *Nat. Commun.*, 2015, 6938.
- T. Dougherty, C. Gomer, B. Henderson, G. Jori, D. Kessel, M. Korbelik, J. Moan and Q. Peng, Photodynamic Therapy, *J. Natl. Cancer Inst.*, 1998, **12**, 889–905.
- G. Tian, W. Ren, L. Yan, S. Jian, Z. Gu, L. Zhou, S. Jin, W. Yin, S. Li and Y. Zhao, Red-Emitting Upconverting Nanoparticles for Photodynamic Therapy in Cancer Cells Under Near-Infrared Excitation, *Small*, 2013, **11**, 1929–1938.
- T. Wen, Y. Zhou, Y. Guo, C. Zhao, B. Yang and Y. Wang, Color-tunable and single-band red upconversion luminescence from rare-earth doped Vernier phase ytterbium oxyfluoride nanoparticles, *J. Mater. Chem. C*, 2016, **4**, 684–690.
- J. Zeng, J. Su, Z. Li, R. Yan and Y. Li, Synthesis and Upconversion Luminescence of Hexagonal-Phase NaYF<sub>4</sub>:Yb,Er<sup>3+</sup> Phosphors of Controlled Size and Morphology, *Adv. Mater.*, 2005, **17**, 2119–2123.
- J. Boyer, F. Vetrone, L. A. Cuccia and J. A. Capobianco, Synthesis of Colloidal Upconverting NaYF<sub>4</sub> Nanocrystals Doped with Er<sup>3+</sup>, Yb<sup>3+</sup> and Tm<sup>3+</sup>, Yb<sup>3+</sup> via Thermal Decomposition of Lanthanide Trifluoroacetate Precursors, *J. Am. Chem. Soc.*, 2006, **128**, 7444–7445.
- J. Shan, X. Qin, N. Yao and Y. Ju, Synthesis of Monodisperse Hexagonal NaYF<sub>4</sub>:Yb, Ln (Ln = Er, Ho and Tm) Upconversion Nanocrystals in TOPO, *Nanotechnology*, 2007, **18**, 445607.
- Z. Li and Y. Zhang, An Efficient and User-friendly Method for the Synthesis of Hexagonal-phase NaYF<sub>4</sub>:Yb, Er/Tm Nanocrystals with Controllable Shape and Upconversion Fluorescence, *Nanotechnology*, 2008, **19**, 345606.
- G. Yi, H. Lu, S. Zhao, Y. Ge, W. Yang, D. Chen and L. Guo, Synthesis, Characterization, and Biological Application of Size-Controlled Nanocrystalline NaYF<sub>4</sub>:Yb, Er Infrared-to-Visible Up-Conversion Phosphors, *Nano Lett.*, 2004, **11**, 2191–2196.
- H. Mai, Y. Zhang, L. Sun and C. Yan, Highly Efficient Multicolor Up-Conversion Emissions and Their Mechanisms of Monodisperse NaYF<sub>4</sub>:Yb,Er Core and Core/



- Shell-Structured Nanocrystals, *J. Phys. Chem. C*, 2007, **111**, 13721–13729.
- 27 F. Wang and X. Liu, Upconversion Multicolor Fine-Tuning: Visible to Near-Infrared Emission from Lanthanide-Doped NaYF<sub>4</sub> Nanoparticles, *J. Am. Chem. Soc.*, 2008, **130**, 5642–5643.
- 28 A. Punjabi, X. Wu, A. Tokatli-Apollon, M. El-Rifai, H. Lee, Y. Zhang, C. Wang, Z. Liu, E. M. Chan, C. Duan and G. Han, Amplifying the Red-Emission of Upconverting Nanoparticles for Biocompatible Clinically Used Prodrug-Induced Photodynamic Therapy, *ACS Nano*, 2014, **10**, 10621–10630.
- 29 W. Wei, Y. Zhang, R. Chen, J. Goggi, N. Ren, L. Huang, K. K. Bhakoo, H. Sun and T. T. Y. Tan, Cross Relaxation Induced Pure Red Upconversion in Activator- and Sensitizer-Rich Lanthanide Nanoparticles, *Chem. Mater.*, 2014, **26**, 5183–5186.
- 30 W. Niu, S. Wu and S. Zhang, A Facile and General Approach for the Multicolor Tuning of Lanthanide-ion Doped NaYF<sub>4</sub> Upconversion Nanoparticles within a Fixed Composition, *J. Mater. Chem.*, 2010, **20**, 9113–9117.
- 31 G. Tian, W. Ren, L. Yan, S. Jian, Z. Gu, L. Zhou, S. Jin, W. Yin, S. Li and Y. Zhao, Red-Emitting Upconverting Nanoparticles for Photodynamic Therapy in Cancer Cells Under Near-Infrared Excitation, *Small*, 2013, **11**, 1929–1938.
- 32 S. Ye, G. Chen, W. Shao, J. Qu and P. N. Prasad, Tuning Upconversion through a Sensitizer/activator-isolated NaYF<sub>4</sub> Core/shell Structure, *Nanoscale*, 2015, **7**, 3976–3984.
- 33 G. Tian, Z. Gu, L. Zhou, W. Yin, X. Liu, L. Yan, S. Jin, W. Ren, G. Xing, S. Li and Y. Zhao, Mn<sup>2+</sup> Dopant-Controlled Synthesis of NaYF<sub>4</sub>:Yb/Er Upconversion Nanoparticles for in vivo Imaging and Drug Delivery, *Adv. Mater.*, 2012, **24**, 1226–1231.
- 34 J. Wang, F. Wang, C. Wang, Z. Liu and X. Liu, Single-Band Upconversion Emission in Lanthanide-Doped KMnF<sub>3</sub> Nanocrystals, *Angew. Chem., Int. Ed.*, 2011, **50**, 10369–10372.
- 35 D. Chen, L. Lei, R. Zhang, A. Yang, J. Xu and Y. Wang, Intrinsic Single-Band Upconversion Emission in Colloidal Yb/Er(Tm):Na<sub>3</sub>Zr(Hf)F<sub>7</sub> Nanocrystals, *Chem. Commun.*, 2012, **48**, 10630–10632.
- 36 J. Song, G. Wang, S. Ye, Y. Tian, M. Xiong, D. Wang, H. Niu and J. Qu, Lanthanide-doped Na<sub>3</sub>ZrF<sub>7</sub> upconversion nanoparticles synthesized by a facile method, *J. Alloys Compd.*, 2016, **658**, 914–919.
- 37 M. Wu, E. Song, Z. Chen, S. Ding, S. Ye, J. Zhou, S. Xu and Q. Zhang, Single-band red upconversion luminescence of Yb<sup>3+</sup>–Er<sup>3+</sup> via nonequivalent substitution in perovskite KMgF<sub>3</sub> nanocrystals, *J. Mater. Chem. C*, 2016, **4**, 1675–1684.
- 38 G. Chen, H. Liu, G. Somesfalean, H. Liang and Z. Zhang, Upconversion Emission Tuning from Green to Red in Yb<sup>3+</sup>/Ho<sup>3+</sup>-codoped NaYF<sub>4</sub> Nanocrystals by Tridoping with Ce<sup>3+</sup> Ions, *Nanotechnology*, 2009, **20**, 385704.
- 39 Y. Wang, G. Liu, L. Sun, J. Xiao, J. Zhou and C. Yan, Nd<sup>3+</sup>-Sensitized Upconversion Nanophosphors: Efficient In Vivo Bioimaging Probes with Minimized Heating Effect, *ACS Nano*, 2013, **7**, 7200–7206.
- 40 X. Li, R. Wang, F. Zhang, L. Zhou, D. Shen, C. Yao and D. Zhao, Nd<sup>3+</sup> Sensitized Up/Down Converting Dual-Mode Nanomaterials for Efficient In-vitro and In-vivo Bioimaging Excited at 800 nm, *Sci. Rep.*, 2013, **3**(3536), 1–4.
- 41 Q. Zhan, J. Qian, H. Liang, G. Somesfalean, D. Wang, S. He, Z. Zhang and S. Andersson-Engels, Using 915 nm Laser Excited Tm<sup>3+</sup>/Er<sup>3+</sup>/Ho<sup>3+</sup>-Doped NaYbF<sub>4</sub> Upconversion Nanoparticles for in Vitro and Deeper in Vivo Bioimaging without Overheating Irradiation, *ACS Nano*, 2011, **5**, 3744–3757.
- 42 J. Shen, G. Chen, A. Vu, W. Fan, O. S. Bilsel, C. Chang and G. Han, Engineering the Upconversion Nanoparticle Excitation Wavelength: Cascade Sensitization of Tri-doped Upconversion Colloidal Nanoparticles at 800 nm, *Adv. Opt. Mater.*, 2013, **7**, 644–650.
- 43 X. Xie, N. Gao, R. Deng, Q. Sun, Q. Xu and X. Liu, Mechanistic Investigation of Photon Upconversion in Nd<sup>3+</sup>-Sensitized Core–Shell Nanoparticles, *J. Am. Chem. Soc.*, 2013, **135**, 12608–12611.
- 44 X. Huang and J. Lin, Active-core/active-shell nanostructured design: an effective strategy to enhance Nd<sup>3+</sup>/Yb<sup>3+</sup> cascade sensitized upconversion luminescence in lanthanide-doped nanoparticles, *J. Mater. Chem. C*, 2015, **3**, 7652–7657.
- 45 D. Chen, L. Liu, P. Huang, M. Ding, J. Zhong and Z. Ji, Nd<sup>3+</sup>-Sensitized Ho<sup>3+</sup> Single-Band Red Upconversion Luminescence in Core–Shell Nanoarchitecture, *J. Phys. Chem. Lett.*, 2015, **6**, 2833–2840.
- 46 Y. Zhang, J. Lin, V. Vijayaragavan, K. K. Bhakoo and T. T. Y. Tan, Tuning sub-10 nm Single-phase NaMnF<sub>3</sub> Nanocrystals as Ultrasensitive Hosts for Pure Intense Fluorescence and Excellent T<sup>1</sup> Magnetic Resonance Imaging, *Chem. Commun.*, 2012, **48**, 10322–10324.
- 47 Z. Wang, J. Feng, S. Song, Z. Sun, S. Yao, X. Ge, M. Pang and H. Zhang, Pure and Intense Orange Upconversion Luminescence of Eu<sup>3+</sup> from the Sensitization of Yb<sup>3+</sup>–Mn<sup>2+</sup> Dimer in NaY(Lu)F<sub>4</sub> Nanocrystals, *J. Mater. Chem. C*, 2014, **2**, 9004–9011.
- 48 J. Liu, N. Li, R. Wu, Y. Zhao and Q. Zhan, Sailing He. Sub-5-nm lanthanide-doped ZrO<sub>2</sub>@NaYF<sub>4</sub> nanodots as efficient upconverting probes for rapid scanning microscopy and aptamer-mediated bioimaging, *Opt. Mater. Express*, 2015, **5**, 1759–1771.
- 49 F. Vetrone, R. Naccache, V. Mahalingam, C. G. Morgan and J. A. Capobianco, The Active-Core/Active-Shell Approach: A Strategy to Enhance the Upconversion Luminescence in Lanthanide-Doped Nanoparticles, *Adv. Funct. Mater.*, 2009, **19**, 2924–2929.

